Temperature-driven polar anchoring transitions in nematic liquid crystals: computer simulations

B. Lin, P. Taylor

J. Phys. II France 4 (1994) 825–836 MAY 1994, PAGE 825

Classification
Physics Abstracts
61.30

Temperature-driven polar anchoring transitions in nematic liquid crystals: computer simulations

B. Lin and P. L. Taylor

Department of Physics, Case Western Reserve University Cleveland, OH 44106-7079, U.S.A.

(Received 18 June 1993, revised 25 January 1994, accepted 3 February 1994)

Abstract . — Using a collective inverted-pendulum model, we have performed computer simulations of temperature-driven anchoring transitions in nematic liquid crystals. Behavior reminiscent of some of the experimentally observed anchoring transitions was obtained in our simulations. We have thus shown that anchoring transitions can be induced by the thermal motion of the substrate. These effects, which originate in molecules in direct contact with the substrate, then propagate into the bulk of the liquid crystal.

1. Introduction.

Anchoring transitions induced by changes in temperature have been observed in several experiments [1-6]. Two types of temperature-driven polar anchoring transitions have been reported. On free surfaces of N-(p-methoxybenzylidene)-p-n-butylaniline (MBBA) and N-(p-ethoxybenzylidene)-p-n-butylaniline (EMMA), anchoring transitions of liquid-crystal molecules from a tilted alignment to a homeotropic one were found [1] as the temperature was increased. Similar transitions were reported [2, 3] in systems of liquid crystal on hydrophilic substrates (glass and quartz) coated with an amphiphilic monolayer (lecithin, cephalin or fatty acid). Another type of polar behavior has been observed in both MBBA [4] and various types of cyanobiphenyl (nCB) [5, 6] when they were on substrates coated with emissions from charred paper and with fluorocarbon polymer respectively. In these systems the director orientation changed from the tilted to the homeotropic and then back to the tilted alignment. In both types of system, the transition from tilted to homeotropic alignment was found to occur gradually over a fairly broad temperature interval, while the transition from homeotropic to tilted alignment appeared quite abrupt.

A different kind of anchoring transition — the torsion anchoring transition, where the director orientation changes on the substrate plane — has been recently observed and investigated [7, 8] in systems of cyanobiphenyl liquid crystals on mica. Both continuous and first-order transitions of this adsorption-driven anchoring transition were observed. The temperature de-

pendence of the anchoring energy of the in-plane director-orientation of 5CB on SiO treated film had been reported earlier [9].

On the theoretical side, there have been several studies of surface free energy and nematic anchoring. Using Landau-de Gennes theory, Ken and Sullivan [10] applied a one-order-parameter approximation to a nematic fluid on a smooth substrate. They obtained a phase diagram of nematic homeotropic and planar orientations in the parameter space of coefficients of the Landau free energy. For nematic liquid crystals at a free surface, Kimura and Nakano [11] calculated the surface tension using a mean field approximation with both attractive and hard-core repulsive intermolecular interactions. Minimizing the surface tension, they found that the hard-core repulsion favors the homeotropic alignment while the attraction stabilizes the planar alignment. Tjipto-Margo and Sullivan [12] used molecular perturbation theory and the Landau-de Gennes approximation to study the orientational alignment at the free nematic-vapor interface by using the Gay-Berne model intermolecular potential. They found a homeotropic preferred anchoring at the interface. Teixeira and Sluckin [13] used a mean field approximation to the Helmholtz free energy functional of a nematic liquid to derive a simpler Landau-de Gennes free energy functional and considered the cases of a liquid crystal (LC) in contact with an anisotropic solid substrate, a LC in contact with an immiscible isotropic medium, and a binary LC mixture on an anisotropic solid substrate. For these three cases they obtained the anchoring phase diagram of planar and homeotropic alignments in the parameter space of the two coefficients of the Landau-de Gennes free energy, which are functions of temperature, and, for the latter two cases, of composition. They also considered surface absorption and found anchoring transitions of planar to homeotropic alignments occur as the concentration is changed. This transition was found to be almost temperature-independent, and thus in accord with that observed by Bechhoefer *et al.* [7, 8].

A phenomenological theory was considered by McMullen [14] to discuss the interfacial polar ordering of liquid crystals. The tilt angle θ_t can be other than 0° or 90° because the molecules at the interface lack up-down symmetry. Using a pseudo-molecule model, Barbero *et al.* [15] showed that the anchoring energy is contributed by two interactions: nematic-nematic and nematic-substrate. The tilt angle and anchoring transitions as a function of temperature were analyzed with a phenomenological approach.

A version of Onsager theory studied by Holyst and Poniewierski [16] showed that the hard-core interaction alone makes the tilt angle of a nematic at the nematic-isotropic interface 60°. A similar consideration by Sharlow and Gelbart [17] of a nematic on a solid wall showed, however, that the excluded-volume effect will align the nematic parallel to the wall. When there is an adsorption energy favoring the normal alignment, the transition to the homeotropic anchoring is possible as temperature is lowered. Another possible effect on anchoring transitions was recently proposed by Barbero and Durand [18]. Using the temperature dependence of the scalar order-parameter S and a continuum theory, they showed that the mixed splay-bend curvature elasticity K_{13} could be a cause of the temperature-driven anchoring transitions.

Although many theories have been proposed and studied, a microscopic theory of the mechanism of temperature-driven anchoring transitions that directly describe the microscopic effect of temperature has for the most part been lacking. In previous papers [19, 20], we have suggested a possible microscopic model for polar anchoring transitions. In this paper we extend the previous model to make it a more realistic description of a nematic liquid crystal. Instead of considering a single-molecule or monolayer system, we study a bulk liquid crystal with an interface having an isotropic substrate. The equations of motion are obtained for each molecule and these dynamic equations are then solved numerically.

2. The model.

When a substrate in contact with a liquid crystal is isotropic, the orientation of the director in the liquid crystal will not depend on the azimuthal angle but only on the polar angle θ (Fig. 1). Thus as an approximation we build a two-dimensional model, as shown in figure 1, to represent the system of a nematic liquid crystal on an isotropic substrate. The z direction is normal to the substrate. The molecules are arranged in a triangular lattice in the x-z plane corresponding to close packing in the liquid crystal.

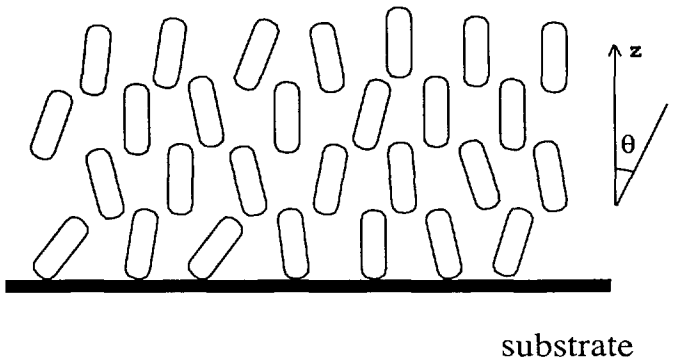

Fig. 1. — Schematic of a model for a bulk liquid crystal having an interface with an isotropic substrate.

The molecules of the first monolayer are in direct contact with the substrate, and are subject to the thermal vibrations of the substrate [19, 20]. The vertical vibration of the anchored base of molecule j in this layer is taken to be of the simple harmonic form

$$z_j(t) = a_j \cos(\Omega t + \eta_j), \tag{1}$$

where a_j is the amplitude of the vibration, Ω the frequency of the characteristic phonon mode of the substrate, and η_j a random phase. A single frequency Ω is used since, as in our calculations discussed in previous papers [19, 20], this approximation gives basically the same results as the use of a complete phonon spectrum. The amplitudes a_j were chosen at random in the range $0.89\bar{a} < a_j < 1.11\bar{a}$, with $\bar{a}$ the average amplitude. The first-layer molecules are also subject to another physical constraint: they can only rotate in the range $-\frac{1}{2}\pi < \theta < \frac{1}{2}\pi$. The intermolecular interactions between the substrate and the molecules in direct contact with it give rise to the anchoring potential on each of the first-layer molecules. We assume the Rapini-Papoular form [21] for this anchoring potential function. For homeotropic anchoring, the molecular anchoring potential $w(\theta)$ is taken to be

$$w(\theta) = \frac{1}{2} w_0 \sin^2 \theta, \tag{2}$$

where w_0 is the anchoring energy per molecule and is positive. For planar anchoring, w_0 is negative.

In the bulk, each molecule is assumed to interact with its six neighbors. The molecules in the first layer and in the uppermost layer, however, have four neighbors with which to interact.

We will use $\theta_{i,j}$ to identify molecules, where the first subscript i indicates layers and the second subscript j is the position index in a layer. We assume the interaction potential between any two neighboring molecules to be of the form

$$p(\theta_{i,j}, \theta_{i'j'}) = \lambda \sin^2(\theta_{i,j} - \theta_{i'j'}), \tag{3}$$

where λ is an interaction constant. This expression reflects the property of neighboring molecules in a nematic liquid crystal to tend to align in the same direction. Finally, the viscosity is taken into account by means of a damping torque

$$\tau_{\mathrm{d}} = -\gamma \frac{\mathrm{d}\theta}{\mathrm{d}t}, \tag{4}$$

where γ is the damping coefficient.

A classical Lagrangian for this assembly of molecules can be obtained from equations (1-3) and written as

$$\mathcal{L} = \sum_{i,j} \left[\frac{1}{24} m l^2 \left(\frac{\mathrm{d}\theta_{i,j}}{\mathrm{d}t} \right)^2 + \frac{m}{2} \left(\frac{l}{2} \cos\theta_{i,j} \frac{\mathrm{d}\theta_{i,j}}{\mathrm{d}t} \right)^2 + \frac{m}{2} \left[-\frac{l}{2} \sin\theta_{i,j} \frac{\mathrm{d}\theta_{i,j}}{\mathrm{d}t} + \frac{\mathrm{d}z_j}{\mathrm{d}t} \delta_{i,1} \right]^2 - w(\theta_{i,j}) \delta_{i,1} - \sum_{k,l} \lambda \sin^2(\theta_{k,l} - \theta_{i,j}) \right], \tag{5}$$

where each molecule is assumed to be in the form of a uniform rod of length l and mass m, and $w(\theta_{i,j})$ is given by equation (2). The summation of k, l is over the six neighbors of molecule $\theta_{i,j}$ except on the first and the uppermost layers, where the summation is over four neighbors.

The equations of motion for the system of size $p \times q$ can be derived from equation (5). We have

$$\begin{cases} \dfrac{\mathrm{d}^2\theta_{1,j}}{\mathrm{d}\tau^2} = -\dfrac{1}{2} w_0' \sin 2\theta_{1,j} - \dfrac{3}{2} \left(\dfrac{a_j}{l} \right) \cos(\tau + \eta_j) \sin\theta_{1,j} \\ \qquad\qquad + \displaystyle\sum_{(k,l)} \lambda' \sin 2(\theta_{k,l} - \theta_{1,j}) - \gamma' \frac{\mathrm{d}\theta_{1,j}}{\mathrm{d}\tau}, \\ \dfrac{\mathrm{d}^2\theta_{i,j}}{\mathrm{d}\tau^2} = \displaystyle\sum_{<k,l>} \lambda' \sin 2(\theta_{k,l} - \theta_{i,j}) - \gamma' \frac{\mathrm{d}\theta_{i,j}}{\mathrm{d}\tau}, \quad i = 2, 3, \cdot \quad, q-1, \\ \dfrac{\mathrm{d}^2\theta_{q,j}}{\mathrm{d}\tau^2} = \displaystyle\sum_{(k,l)} \lambda' \sin 2(\theta_{k,l} - \theta_{q,j}) - \gamma' \frac{\mathrm{d}\theta_{q,j}}{\mathrm{d}\tau}, \end{cases} \tag{6}$$

where $j = 1, 2, \cdot \quad, p$ and

$$\begin{cases} w_0' = \dfrac{3w_0}{ml^2\Omega^2}, \\ \lambda' = \dfrac{3\lambda}{ml^2\Omega^2}, \\ \gamma' = \dfrac{3\gamma}{ml^2\Omega}. \end{cases} \tag{7}$$

The summation $\sum_{(k,l)}$ has four terms and $\sum_{<k,l>}$ has six, and $\tau \equiv \Omega t$ is a dimensionless time.

Periodic boundary conditions are imposed, so that

$$\begin{cases} \theta_{i,0} = \theta_{i,p} \\ \theta_{i,p+1} = \theta_{i,1}. \end{cases} \tag{8}$$

By representing the dynamics of a nematic liquid crystal on an isotropic substrate by equations (6), we have ignored the positional interactions between liquid crystal molecules. We are thus making the implicit assumption that the translational motion will not significantly affect the anchoring transitions.

3. Magnitudes and numerical calculations.

Before embarking on the simulations, let us estimate some typical values of w_0', λ' and γ'. Taking nCB as an example, we have the molecular weight $m \approx 4 \times 10^{-25}$ kg, the length of the rigid part of molecules $l \approx 10^{-9}$ m, the number density $N_v \approx 10^{28}$ m^{-3}, the surface number density $N_s \approx 10^{18}$ m^{-2} and the viscosity $\eta \approx 10^{-3}$ kg m^{-1} s^{-1} [22]. We take the anchoring energy coefficient $W_0 \approx 10^{-5}$ J m^{-2}. The phonon frequency for solids is taken to be $\Omega \approx 5 \times 10^{12}$ s^{-1} and the vibration amplitude $a_j \approx 2 \times 10^{-11}$ m.

The anchoring energy per molecule w_0 can be estimated from W_0 and N_s, giving $w_0 \approx 10^{-23}$ J. The orientational interaction constant λ was obtained using the Maier-Saupe mean field approximation for the potential energy of a molecule and experimental data fitted to coefficients of the potential. We have $\lambda \approx 0.6 \times 10^{-22}$ J. Stokes's formula for the drag force on a sphere moving in a viscous liquid with viscosity η was used to estimate the damping constant γ with the relation $\gamma \approx 0.1\eta/N_v$ which gives $\gamma \approx 10^{-33}$ kg m^2 s^{-1} We therefore have

$$w_0' \approx 10^{-6}, \quad \lambda' \approx 10^{-5}, \quad \gamma' \approx 10^{-3} \tag{9}$$

As an estimate for the temperature at which we simulate the liquid crystal system, we use the relation

$$k_B T = ma^2\Omega^2. \tag{10}$$

With the numbers given above, the temperature T is about 300 K.

The coupled differential equations (6) were solved numerically in a system of 50×6 molecules. Some larger sample calculations on systems of size 80×9 were also performed, but no significant difference was found. In making the numerical simulations, we calculate the director direction d as a function of the average vibration amplitude $\bar{a}$ given by

$$\bar{a} = \frac{1}{p}\sum_{j=1}^{p} a_j \ , \tag{11}$$

where p is the number of molecules in direct contact with the substrate, and

$$d = \langle \bar{\theta} \rangle \tag{12}$$

with $\bar{\theta}$ the time-averaged angle θ and $\langle \theta \rangle$ the molecule average. Caution was exercised when making the ensemble average since the molecules are non-polar. The order parameter S is also calculated as a function of $\bar{a}$ through the relation

$$S = \langle 2\cos^2\alpha - 1 \rangle = \int f(\alpha)(2\cos^2\alpha - 1)\mathrm{d}\alpha, \tag{13}$$

where α is the angle between the time-averaged molecular axis and the director, and $f(\alpha)$ the angle distribution function. This is the two-dimensional version of the general three-dimensional scalar order parameter [23]. For a completely ordered system, $f(\alpha) = \frac{1}{2}[\delta(\alpha) + \delta(\pi - \alpha)]$ and hence $S = 1$. For a system of totally random orientation, $f(\alpha) = 1/2\pi$ and $S = 0$. In actual discrete systems, equation (13) is written as

$$S = \frac{1}{N}\sum_{i=1}^{N}(2\cos^2\alpha_i - 1), \tag{14}$$

where $N = pq$ is the total number of molecules in the system. In setting initial conditions for the equations of motion (6), we set the phase η_j of the thermal vibrations to random numbers so that no particular phase relation existed between molecules. For planar anchoring systems, the initial molecular orientations were set to be randomly and uniformly distributed between 80° and 100°, and −80° and −100° so that the director is at 90°. The orientations of the substrate layer were set to be ± 90° randomly. All angles are measured from the normal to the substrate. For homeotropic anchoring, the initial angle configuration was within the range −10° to 10°. After each temperature increase, we allowed the system to relax to its equilibrium in about 3000 cycles of vibration period before collecting data for averaging. Typically about 10^4 cycles of data were used for calculations. The time step in the numerical calculations was 0.1 of a period.

4. Results.

4.1 PLANAR ANCHORING. — We start by considering a planar anchoring system. There are two possible anchoring transitions as the temperature (proportional to $(\bar{a}/l)^2$) is increased. A typical behavior of the director in the planar-homeotropic transition is as shown in figure 2a. The system director reorients to a homeotropic alignment at a relatively low temperature and stays in this alignment for a range of temperature. The second anchoring transition, shown in figure 2b, occurs at a higher temperature at which the director undergoes a re-entrance to the planar alignment. The parameters used in figures 2 are $w_0'^{(1)} = 5 \times 10^{-6}$ and $w_0'^{(2)} = 2 \times 10^{-6}$ which correspond to $W_0^{(1)} = 1.25 \times 10^{-5}$ J m^{-2} and $W_0^{(2)} = 5 \times 10^{-6}$ J m^{-2} respectively, and $\lambda' = 5 \times 10^{-6}$ and $\gamma' = 3 \times 10^{-3}$ We see in figure 2a that the value of $\bar{a}/l$ necessary for the planar-homeotropic transition to occur is then only about 0.01, and would be found at around room temperature. The $\bar{a}/l$ for the reentrant transition from the homeotropic to the planar alignment, however, is much larger, and does not lie within the physically achievable regime. This suggests that the effect of substrate vibration may not be a dominant factor in this reentrant transition or that effects not present in this model may give important contributions to this transition.

We have, for example, ignored the correlations between motions of substrate atoms, and hence underestimated the effect of substrate vibrations; this will result in an overestimate of the magnitude of $\bar{a}/l$ required for the transition.

In a more sophisticated model it would be possible for the clearing temperature to be reached before the re-entrant anchoring transition could happen, so that only the planar-to-homeotropic transition would be observed. Our model does not exhibit a clearing transition because the bulk of the sample is not in contact with a thermal reservoir.

Another feature of figures 2 is seen by examining the rate of approach to the homeotropic alignment and the rate of departure from it at the two transitions in the region where the d

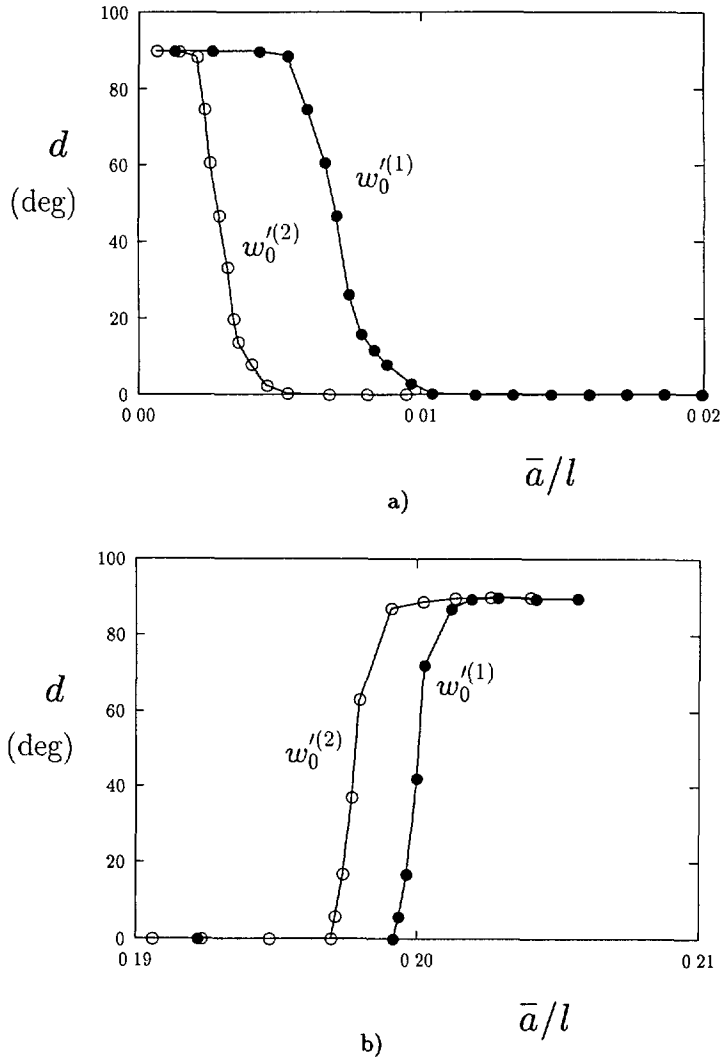

Fig. 2. — Anchoring transitions for a planar anchoring system are shown in these plots, which give the deviation d of the director from the substrate normal. Here $\gamma' = 3 \times 10^{-3}$, $\lambda' = 5 \times 10^{-6}$ and $w_0'^{(1)} = 5 \times 10^{-6}$ and $w_0'^{(2)} = 2 \times 10^{-6}$. In case (a), planar-homeotropic anchoring transitions are shown. In case (b), the anchoring transition is from homeotropic to planar.

is small. While the initial change from the planar alignment is abrupt, the approach to $d = 0$ appears smooth and continuous over the last few degrees [Fig. 2a]. In contrast, the departure from homeotropic alignment appears sharp, with a discontinuous slope at a well defined transition temperature [Fig. 2b]. This type of behavior is in accord with some experimental findings [1-2, 4-5].

We can demonstrate that the mechanism of the temperature-driven anchoring transitions is driven by the substrate thermal vibrations by examining the motion layer by layer. Figure 3 shows the orientations of the layer directors on different layers for a system that differs from

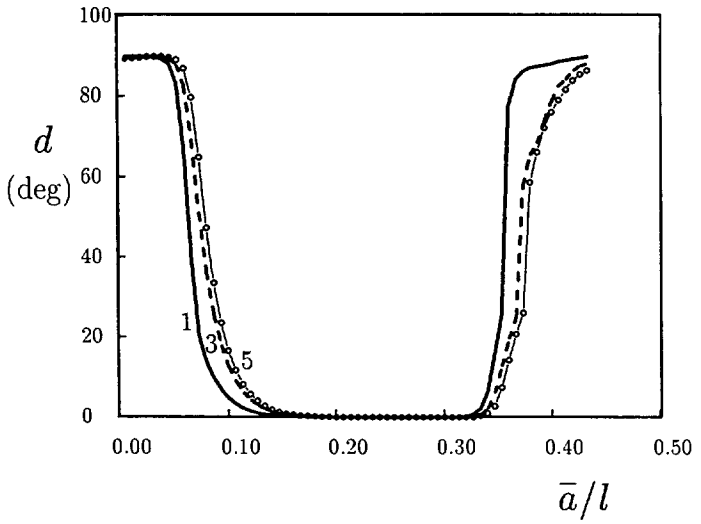

Fig. 3. — The reorientation of molecules first occurs on the layer of molecules in contact with substrate and then propagates into the bulk. The labels on the curves indicate layer number. The parameters are the same as in figures 2 except that $w_0' = 2 \times 10^{-3}$

that of figure 2 in that now $w_0' = 2\times10^{-3}$. (This would be the case for strong anchoring W_0 and small substrate frequency Ω.) We see that in both the planar-homeotropic and the homeotropic-planar transitions, the first-layer director leads the orientation change. Quick propagation of the orientation change into the bulk leads to the anchoring transitions of the whole system. In this figure we used large values of w_0' for the purpose of illustrating clearly both planar-homeotropic and homeotropic-planar transitions in the same figure. The $\bar{a}/l$ magnitude of 0.1~0.2 for the transitions would then be too large to be physically realized.

The order parameter S defined in equation (14) is shown in figure 4. It is near unity when the system is in a planar or a homeotropic orientation, and takes on lower values as the system is in transition from one state to another. This behavior of the order parameter reflects the fact that anchoring transitions are transitions between ordered states. The more gradual anchoring change from planar to homeotropic states than from homeotropic to planar states is also apparent in figure 4 in the larger range of $\bar{a}/l$ over which disorder is present.

As we can see from the system's equations of motion (6), the nature of the anchoring transitions and the ranges of temperature for planar and homeotropic alignments depend on the parameters w_0', λ' and γ'. A stronger anchoring energy will shift the transition points for both transitions to higher temperatures (Fig. 2), but a system with lower anchoring energy has a larger temperature range of homeotropic alignment. This can be understood by realizing that a stronger planar anchoring energy will require a higher vibrational energy to destabilize the system from the planar alignment. This pattern of behavior was seen in the simple one-molecule and single-layer models [19, 20].

The interaction potential has the effect of enhancing the effect of the thermal vibrations. When the anchoring energy w_0' and the damping coefficient γ' are kept unchanged, an increase in the interaction constant λ' will make both transitions occur at lower temperatures. This dependence probably stems from two causes, the first being that the random phases and amplitudes of the first-layer vibrations are effectively replaced in the interacting system by

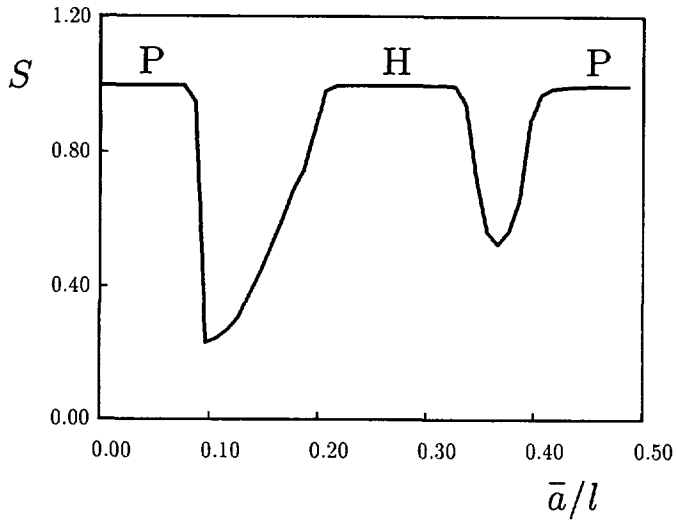

Fig. 4. — Order parameter S as a function of $\bar{a}/l$ in a planar anchoring system with $w_0' = 6 \times 10^{-3}$, $\gamma' = 3 \times 10^{-3}$ and $\lambda' = 5 \times 10^{-6}$ The regions labeled P indicate planar alignment and H homeotropic alignment.

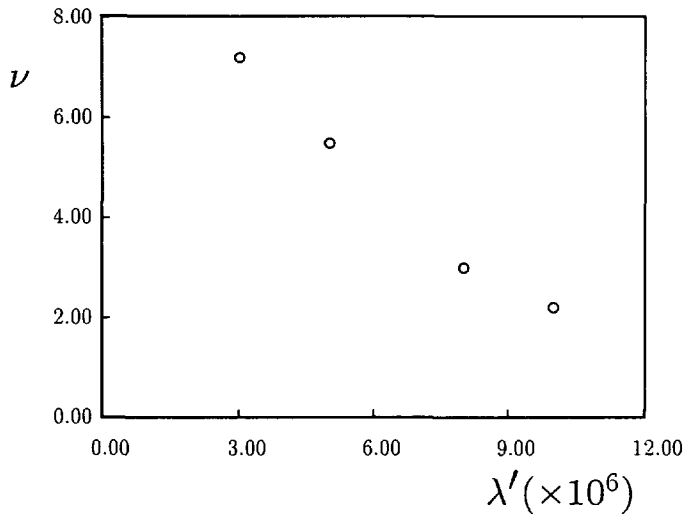

Fig. 5. — The dependence of the scaling exponent ν on the interaction constant λ'. Here $w_0' = 6 \times 10^{-3}$ and $\gamma' = 3 \times 10^{-3}$

a mean amplitude and phase. The second cause could be that a stronger interaction will strengthen the propagation of the reorientation process from the first layer into the bulk, and therefore make the whole system reorient earlier. Damping plays a different role in the anchoring transitions. Its presence is necessary to dissipate some thermal energy, but if the damping is too strong, the reorientation energy will be dissipated too greatly, and the anchoring

transition will be prevented.

The temperature dependence of the approach to the homeotropic orientation appears to follow a power law. The angle, d, between director and substrate normal varies as a power, ν, of the difference between the temperature T and the critical temperature T_c at which d vanishes, so that

$$d = C(T_c - T)^{\nu}, \tag{15}$$

where C is a constant. The critical exponent ν appears to be independent of the anchoring energy w_0', although it is a function of the interaction and damping constants, λ' and γ'. For $\lambda' = 0.5 \times 10^{-5}$ and $\gamma' = 0.3 \times 10^{-2}$, our calculations give $\nu \approx 5.5$ for w_0' from 0.5×10^{-3} to 0.2×10^{-1} This typical large value of ν characterizes the behavior of d in the planar-homeotropic transition: the director angle d changes rapidly to some small angle (around 20°) of a tilted alignment and then slowly approaches zero (homeotropic alignment). The exponent ν, however, changes when the interaction constant λ' is changed. Figure 5 shows that ν decreases as λ' is increased.

4.2 HOMEOTROPIC ANCHORING. — For a homeotropic anchoring system, our simulations also show anchoring transitions when the substrate oscillates with a single monochromatic frequency. In this case, the director orientation, as one would expect, is homeotropic when the thermal vibration is moderate. As in the case of planar anchoring, increasing thermal vibration of the substrate destabilizes the first-layer molecules and rotates them to a new orientation, and then this reorientation propagates into the inner layers. However, the homeotropic-planar anchoring transition mechanism is rather sensitive to the nature of the spectrum of substrate oscillations. The transition tends to be suppressed when a wide spectrum of frequencies is used

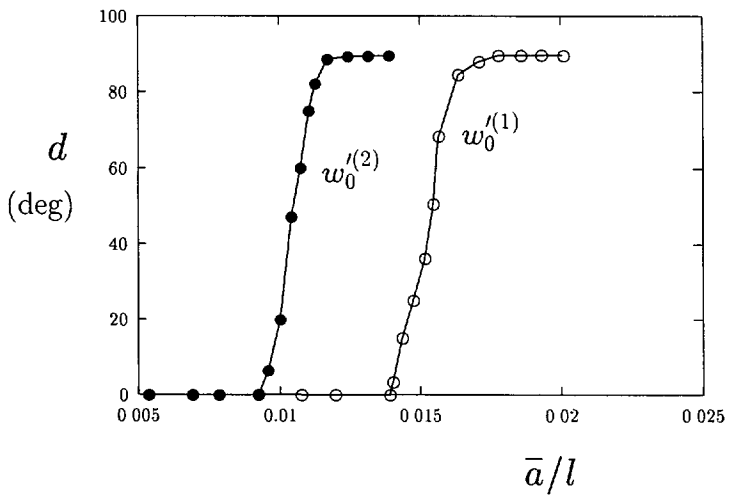

Fig. 6. — Anchoring transitions for a homeotropic anchoring system. Increasing the anchoring energy w_0' decreases the transition temperature. Here $w_0'^{(1)} = 2.4 \times 10^{-1}$ and $w_0'^{(2)} = 2.2\times10^{-1}$ Both curves have $\gamma' = 3 \times 10^{-2}$ and $\lambda' = 1.5 \times 10^{-2}$

to model the phonon dynamics. It thus appears that there is little to be said in the way of general conclusions about this particular process that might be useful in predicting transition temperatures. We do, however, note a significant difference in the effect of the strength of the anchoring. This is illustrated in figure 6, which shows a typical anchoring transition of a homeotropic system. We see that the influence of the anchoring energy is in the opposite direction to that in a planar anchoring system. The anchoring transition temperature *decreases* as the strength of the anchoring energy increases.

For the anchoring transition shown in figure 6 we have chosen two anchoring energies, $W_0^{(1)} = 9.6 \times 10^{-4}$ J m^{-2} and $W_0^{(2)} = 8.8 \times 10^{-4}$ J m^{-2}, and a low substrate frequency of $\Omega = 0.2 \times 10^{12}$ rad s^{-1} The parameters γ and λ are the same as in the planar-anchoring systems.

5. Conclusions and discussions.

We have constructed a microscopic model for temperature-driven polar anchoring transitions in nematic liquid crystals. Both planar and homeotropic anchorings have been considered. We obtained in our model a sequence of anchoring transitions from planar to homeotropic and reentrance back to planar alignments for initially planar anchoring systems, and transitions of homeotropic to planar alignments for certain types of homeotropic anchoring system. Our simulations show that substrate thermal vibration is a driving force for the anchoring transitions. The reorientations of molecules first occur at the layer where molecules have direct contact with the substrate; this change of director orientation is then propagated into the bulk through intermolecular interactions. The polar anchoring transitions of planar to homeotropic alignments and the sequence of transitions of planar-homeotropic-planar alignments formed in the model bear some resemblance to those that have been reported in experiments. The continuous change of director orientation in the planar-to-homeotropic alignment transition and the more abrupt change in the homeotropic-to-planar transition in our model are also in general agreement with experimental findings. The substrate vibrational amplitude for the homeotropic-to-planar transition, however, is greater than is physically realizable, which suggests that the effect of substrate vibration may not dominate in the reentrant transition.

The anchoring transition from homeotropic to planar with increasing temperature in an initially homeotropic anchoring system, seen in our simulations when the substrate spectrum was modeled by using a single frequency, has also been reported in experiments, although this behavior has not been studied as extensively as the planar-to-homeotropic transition. In a system of the liquid crystal butoxybenzylidene octylaniline, also known as (4O.8), sandwiched between two smooth float-glass plates [24], and also in a system of the liquid crystal ZLI2806 sandwiched between glass plates coated with SiO_x and lecithin [25], homeotropic-to-planar anchoring transitions have been observed as the temperature was increased. It may be the case that these particular surfaces vibrate with a more nearly monochromatic phonon spectrum than do some alternative surfaces.

Finally, we point out some of the shortcomings of the simulations described here. The arrays used were confined to two dimensions, rather than the three dimensions of the real world of liquid crystals. Secondly, the phases of the substrate motion at the individual anchoring points were taken to be random, thus ignoring the expected correlations between motion at neighboring sites. The effects of both of these approximations are likely to be an underestimation of the collective motions that would be likely to sharpen the transition processes. Thirdly, the individual molecules were not allowed any translational degrees of freedom. The effect of this omission is less clear, but is probably in the opposite direction from the other factors, and thus

likely to broaden the predicted temperature range over which the transitions take place. It is clear that a more careful treatment of the microscopic dynamics of liquid crystal anchoring is necessary before a satisfactory understanding of these complex phenomena can be attained.

Acknowledgements.

This work was supported by the National Science Foundation at the ALCOM Science and Technology Center funded by grant number DMR89-20147.

References

[1] Chiarelli P., Faetti S. and Fronzoni L., *J. Phys. France* **44** (1983) 1061.
[2] Hiltrop K. and Stegemeyer H., Liquid crystals and Ordered Fluids, A.C. Griffin and J.F. Johnson Eds. vol. **4** (Plenum, New York, 1984) p.515.
[3] Di Lisi G.A., Rosenblatt C., Griffin A.C. and Hari U., *Liq. Cryst.* **7** (1990) 353.
[4] Ryschenkow G. and Kleman M., *J. Chem. Phys.* **64** (1976) 404.
[5] Birecki H., same as reference [2], p.853.
[6] Patel J.S. and Yokoyama H., *Nature* **362** (1993) 525.
[7] Bechhoefer J., Jérome B. and Pieranski P., *Phys. Rev. A* **41** (1990) 3187.
[8] Bechhoefer J., Duvail J-L., Massou L., Jérome B., Hornreich R.M. and Pieranski P., *Phys. Rev. Lett.* **64** (1990) 1911.
[9] Faetti S., Gatti M., Palleschi V. and Sluckin T.J., *Phys. Rev. Lett.* **55** (1985) 1681.
[10] Sen A.K. and Sullivan D.E., *Phys. Rev. A* **35** (1987) 1391.
[11] Kimura H. and Nakano H., *J. Phys. Soc. Jpn* **54** (1984) 1730.
[12] Tjipto-Margo B. and Sullivan D.E., *J. Chem. Phys.* **88** (1988) 6620.
[13] Teixeira P.I.C. and Sluckin T.J., *J. Chem. Phys.* **97** (1992) 1498; *ibid* **97** (1992) 1510.
[14] McMullen W.E., *Phys. Rev. A* **40** (1989) 2649.
[15] Barbero G., Gabbasova Z. and Osipov M.A., *J. Phys. II France* **1** (1991) 691.
[16] Holyst R. and Poniewierski A., *Phys. Rev. A* **38** (1988) 1527 .
[17] Sharlow M.F. and Gelbart W.M., *Liq. Cryst.* **11** (1992) 25.
[18] Barbero G. and Durand G., *Phys. Rev. E* **48** (1993) 1942.
[19] Lin B. and Taylor P.L., *Phys. Lett. A* **172** (1993) 281.
[20] Lin B. and Taylor P.L., Liquid-crystal anchoring transitions induced by thermal motions, to appear in *Liq. Cryst.*
[21] Rapini A. and Papoular M., *J. Phys. Colloq. France* **30** (1969) C4-54.
[22] Kelker H., Handbook of Liquid Crystals (Verlag Chemie, 1980);
Chandrasekhar S., Liquid Crystals (Cambridge University Press, 1980).
[23] de Gennes P.G., The Physics of Liquid Crystals (Clarendon Press, 1974) p.24.
[24] Känel H.V., Litster J.D., Melngailis J. and Smith H.I., *Phys. Rev. A* **24** (1981) 2713.
[25] Flatischler K., Komitov L., Lagerwall S.T., Stebler B. and Strigazzi A., *Mol. Cryst. Liq. Cryst.* **198** (1991) 119.